Carlos LEMOS ANTUNES[1], Tony ALMEIDA[2], Nélia RAPOSEIRO[1]

RIANDA Research (1), DEEC/FCT - University of Coimbra (2)

Producing a Regular Thermal Lesion Volume on a Cholangiocarcinoma Considering a Saline-Enhanced RF Ablation

Abstract. *Self-expandable mechanical stents are an effective option for reducing stricture problems of hollow organs, like the bile duct, and so for improving quality of life of the patients. It has been shown that this mechanical device, made out of nitinol, can also be used as a radio frequency ablation electrode for inducing thermal necrosis in the tumorous tissue. However, for the thermal ablation of a cholangiocarcinoma, the volume lesion obtained is not regular. In this work, it is intended to study the thermal lesion obtained considering a saline-enhanced radio frequency ablation. Analysis was performed based on numerical simulation, and results show that it is possible to reduce irregularity of the volume obtained, although convective heat transfer due to blood flow has a significant impact in the final result.*

Streszczenie. *Samo-rozszerzalne mechaniczne stenty stanowią efektywną możliwość redukcji zwężeń wydrążonych organów, takich jak dróg żółciowych, a w konsekwencji do polepszenia jakości życia pacjentów. Zostało pokazane, że to mechaniczne urządzenie, wykonane z nitinolu, może też zostać wykorzystane jako elektroda do ablacji wysokoczęstotliwościowej dla wywołania obumarcia tkanki guzowatej. Jednakże, w przypadku termoablacji raka dróg żółciowych, otrzymana zmiana objętościowa nie jest regularna. W tym artykule przedstawiono badania zmian termicznych, które otrzymano stosując termoablację ze wspomaganiem solnym. Przeprowadzono analizę numeryczną, której wyniki wskazały na możliwość redukcji nieregularności objętościowej , aczkolwiek konwekcyjny przepływ ciepła wynikły z przepływu krwi ma istotny wpływ na wynik końcowy.* ***(Produkowanie regularnych zmian termicznych w raku dróg żółciowych przy stosowaniu termoablacji wysokoczęstotliwościowej ze wspomaganiem solnym).***

Keywords: cholangiocarcinoma, RF ablation, saline-enhanced, finite element method, numerical simulation.
Słowa kluczowe: rak dróg żółciowych, ablacja wysokoczęstotliwościowa, metoda elementów skończonych, symulacja numeryczna

Introduction

Cholangiocarcinoma is an adenocarcinoma of the bile duct which drains bile from the liver into the small intestine. It is the second most common primary hepatic malignancy, and incidence and mortality rates are increasing worldwide [1]. Unfortunately, most patients are diagnosed on an advanced stage of the disease with almost no chances for surgery, the only potentially curative treatment [2]. As nitinol stents can be used to reduce stricture problems of the bile duct [3], these can be also considered as potential electrodes for hyperthermia treatments.

Previous work showed that a stent-based electrode is a feasible solution for radio frequency ablation therapy [4 - 6]. However, the volume of lesion obtained is not regular [7]. The convective heat transfer due to the blood flow in the portal vein and hepatic artery, next to the bile duct, is a major factor for obtaining this irregular volume. In order to obtain a more regular volume of lesion, a previous study for radio frequency thermal ablation considering an infused saline solution in the tumorous tissue was performed [8]. Diffusion of the saline solution across the tumour was not taken into account and so the shape of the lesion induced in the tissue is not totally accurate. Considering the small dimension of the bile duct, and considering that it is important not to injure this organ, it is very significant to obtain a more accurate volume of damaged tissue in order to prevent the destruction of the bile duct.

To overcome the limitations of the previous model, in this work is intended to perform a numerical analysis of a radio frequency ablation procedure using a stent-based electrode and considering a Gaussian function to represent the diffusion of the saline solution across the tumorous tissue. This analysis is performed taking into account different values of concentration for the saline solution as well as different patterns for the saline solution spread across the tumour, from a narrow distribution to a wide one.

Equations

Most commercial generators of radio frequency ablation works between 375 to 480 kHz. At this frequency range, most part of the energy dissipated by the electric probe is through electrical conduction and so quasi-static approximation is valid [9]. Joule heating can be calculated considering a RF voltage applied between the stent-based electrode and the return pad. The electric field across the domain is solved by using Laplace's equation:

$$\nabla \cdot \left[\sigma(T) \nabla V \right] = 0 \tag{1}$$

where ∇ is the gradient operator, $\sigma(T)$ is the electrical conductivity [S/m], which is considered temperature-dependent, and V is the electric potential [V]. The temperature at each point of the domain can be obtained from:

$$\rho c \frac{\partial T}{\partial t} = \nabla \cdot k \nabla T - \omega_b c_b (T - T_b) + Q_m + \\ + \mathbf{J} \cdot \mathbf{E} - \rho_b c_b \mathbf{u}_b \cdot \nabla T \tag{2}$$

where ρ is the density [kg/m^3], ρ_b is the blood density [kg/m^3], c is the specific heat [J/kg·K], c_b is the blood specific heat [J/kg·K], T is the temperature [K], T_b is the blood temperature [K], k is the thermal conductivity [W/m·K], $\mathbf{J}$ is the current density [A/m], $\mathbf{E}$ is the electric field intensity [V/m], Q_m is the energy due to metabolic process [W/m^3], ω_b is the blood perfusion [kg/m^3·s], and $\mathbf{u}_b$ is the velocity of the blood in the blood vessels [m/s]. In the analysis performed, the terms Q_m and $\omega_b c_b (T - T_b)$ were considered insignificant. Finally, the last term of (2) corresponds to a moving heat sink due to the blood flow in the porta vein and hepatic artery. This equation is a modification of the Pennes' equation [10], and it corresponds to the Chen and Holmes model [11].

At each iteration, the voltage through the domain of analysis is calculated from equation (1) and so the distributed heat source $\mathbf{J} \cdot \mathbf{E}$, to be used in (2), is obtained. The temperature distribution is calculated and the electrical conductivity of the tissue, which is temperature-dependent, is recalculated. The steps during the solution of the finite element model started at 0.01 s and they were

subsequently and automatically controlled by the solver software.

Model Geometry

In this work, it was considered a simplified 3D model of the porta hepatis. The 3D model was created considering an external cylinder (liver) with 200 mm diameter and 100 mm height. The bile duct and the portal vein are cylinders of radius 5 mm and the hepatic artery is a cylinder of radius 2 mm [12]. The portal vein and the bile duct are positioned on a circumference of 6 mm radius separated by an angle of 120º. The hepatic artery is located so the distance between the three ducts is the same. Fig. 1 shows the position of the blood vessels and the bile duct. The tumour is represented as a tube of 40 mm length, 5 mm radius and 3 mm thickness, placed in the middle of the bile duct, and represented by the shaded area in Fig. 1.

The electrode is made up of 24 nitinol wires with 0.25 mm diameter. Each wire is a helix of radius 2 mm with a pitch of 25 mm. The whole electrode is 40 mm long, placed inside the tumour. The whole model used in all simulations is presented in Fig. 2.

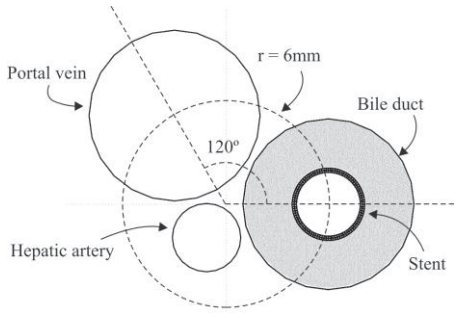

Fig.1. Geometry of the porta hepatis model. Location of the blood vessels and the bile duct

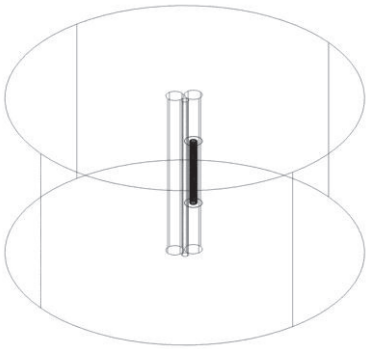

Fig.2. Representation of the model proposed

Material Properties

The material properties used for solving the model considered in this work were obtained from the literature [12 - 15] and they are presented in Table 1 and Table 2. A particular attention should be considered for both electrical conductivities of healthy and tumorous tissues.

As expressed on Table 2, the electrical conductivity of the tumour is considered temperature-dependent and position-dependent. It was considered that a saline solution was injected in the middle portion of the tumour and it diffused symmetrically to both sides of it, considering a Gaussian function. The geometric model created was obtained considering the axis of the tumour parallel to the z-axis and centred at z = 5 so the electrical conductivity will depend on the value of z.

Taking into account the injected saline solution, the electrical conductivity in the middle of the tumour with saline is considered a multiple of the electrical conductivity of the tumour without saline, and it decreases as we move from the middle to the ends of the tumour. Thus, the electrical conductivity can be approximated to:

$$\sigma_t(T,z) = [1+0.02(T-T_{25^\circ\mathrm{C}})]\cdot \cdot\left[\sigma_{\mathrm{tumour}} + \sigma_{\mathrm{saline}} \exp\frac{(z-0.05)^2}{2s^2}\right] \tag{3}$$

where T is the temperature, z is the position on the z-axis (parallel to the axis of the tumour) and s is a measure of how the saline is spread along the axis of the tumour. σ_{tumour} corresponds to the electrical conductivity of the tumorous tissue at 25ºC, with a value of 0.269 S/m, σ_{saline} is the electrical conductivity of the saline, dependent of its concentration. The electrical conductivity of the saline is considered as a multiple of σ_{tumour}, i. e., $\sigma_{\mathrm{saline}} = (ks-1)\,\sigma_{\mathrm{tumour}}$, where $ks \geq 1$ (for $ks = 1$ there is no saline solution, and the conductivity of the tumour is just temperature dependent).

Table 1. Blood vessels characteristics

Blood Vessel	*Diameter* [mm]	*Blood Perfusion* [ml/min]
Vena Cava	10	327.55
Hepatic Artery	4	20.5

Table 2. Material properties

Element	Material	ρ [kg/m^3]	c [J/kg·K]	k [W/m·K]	σ [S/m]
Electrode	Nitinol	6450	840	18	$1\cdot10^8$
Hole	Air	1.202	1	0.025	0
Tissue	Liver	1060	3600	0.512	σ_t(T)
Tumor	Tumor	1060	3600	0.512	σ_t(T, z)
vessels	Blood	1000	4180	0.543	0.667

The parameter s is a measure of how the saline solution spreads along the tumour. A higher value of s corresponds to a wider bell-shaped function, as depicted in Fig. 3. In the present analysis, it was considered three different values of s: $1.7\cdot10^{-3}$, $5\cdot10^{-3}$ and $6.75\cdot10^{-3}$. For these values, the electrical conductivity decreases to 66.6% of its peak value, which is verified at the middle of the tumour, at 0.25, 0.75 and 1 cm away from the middle of the tumour, respectively. Also, it was considered ks varying from 1 (no saline solution) to 5. For example, in Fig. 3, there are presented the curves of the electrical conductivity of the tumour for ks = 2 at 25ºC.

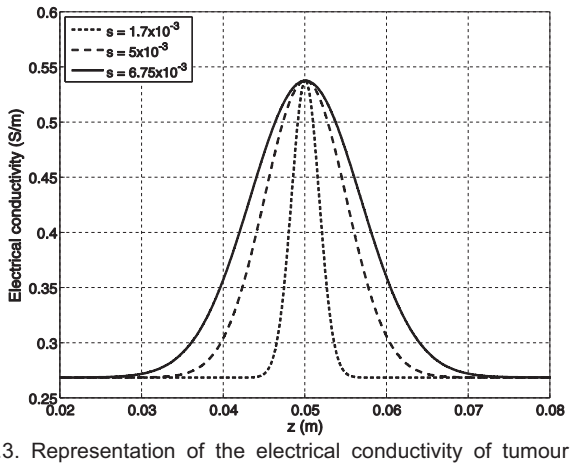

Fig.3. Representation of the electrical conductivity of tumour for ks = 2 at 25ºC

Finally, the electrical conductivity of the tumorous tissue, as well as the electrical conductivity of the liver tissue, were considered temperature dependent, increasing 2%/ºC, and dropping to 0.001 S/m above 100ºC, allowing this way to simulate the electrical insulation verified when gas forms at this temperature value [16]. The electrical conductivity of the liver tissue was set to 0.13 S/m at 25ºC [13].

Model Conditions and Software

For each of the values of s applied in this analysis, ks varied from 1 to 5. Numerical simulations were then performed considering constant source voltages of 20, 22, 24, 26, 28 and 30 volts, making a total of 78 simulations. The external boundary of the model was considered at ground potential (zero volts). The temperature at the external surfaces of the model, the initial temperature of the tissue, and the blood temperature were set to 37ºC.

The stent structure was created in AutoCAD and exported in 3D ACIS format to COMSOL Multiphysics 4.1 (COMSOL, Inc. Burlington, MA, USA). The remaining model was created within COMSOL. All models were solved with PARDISO solver considering a RF ablation procedure of 10 minutes. Each model took an average time of 2.5 hours to solve using a computer with an Intel Core 2 Quad CPU @2.34Ghz, with 8GB of RAM, on a 64 bits platform (Windows Vista).

Results and Discussion

Radio frequency ablation intends to destroy tumorous tissue using heat to induce cellular damage. For a temperature between 50-52ºC, citotoxicity can be achieved in 4 to 6 minutes. Above 60ºC, protein coagulation can be attained almost instantaneously [17]. Taking this into account, volumes enclosed by isothermal surfaces of 50ºC are considered for analysis of the volumes of the lesion achieved in each setting simulated.

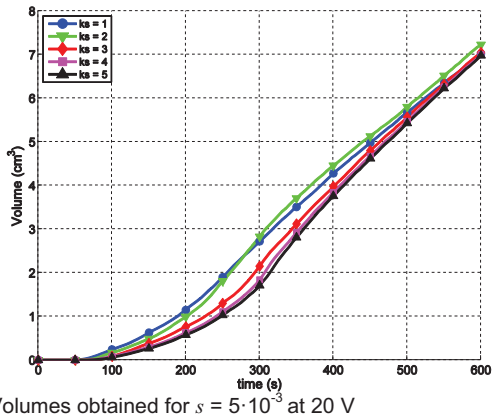

Fig.4. Volumes obtained for $s = 5 \cdot 10^{-3}$ at 20 V

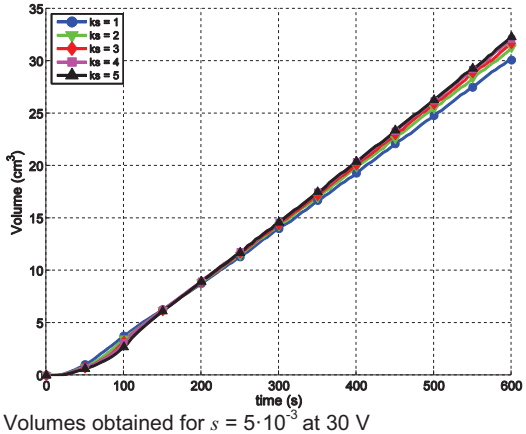

Fig.5. Volumes obtained for $s = 5 \cdot 10^{-3}$ at 30 V

In Fig.4 and Fig.5, there are presented the volumes obtained for $s = 1.7 \cdot 10^{-3}$ and ks varying from 1 to 5, at 20 and 30 V, respectively. As expected, increasing the applied voltage also increases the volume of induced damaged tissue. From these figures, it can be observed that, at 20 V, the volumes obtained are slightly different as ks varies. As the electrical conductivity increases, the volume of damaged tissue obtained is somewhat smaller. However, these values tend to converge as time elapses, and they are very similar after 10 minutes. This behaviour can be observed at every value of applied voltage considered, however the values of volume converge sooner as voltage increases. At 30 V (Fig.5), it can be noticed that values converge close to 170 s. From this point forward, the values of volume start to slightly diverge and the volume obtained is larger for greater values of ks.

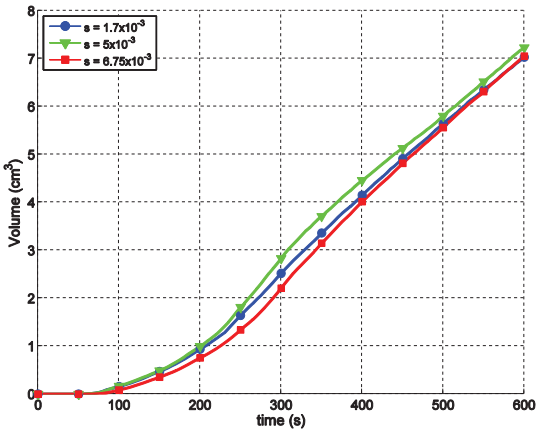

Fig.6. Volumes obtained for $ks = 2$ at 20 V

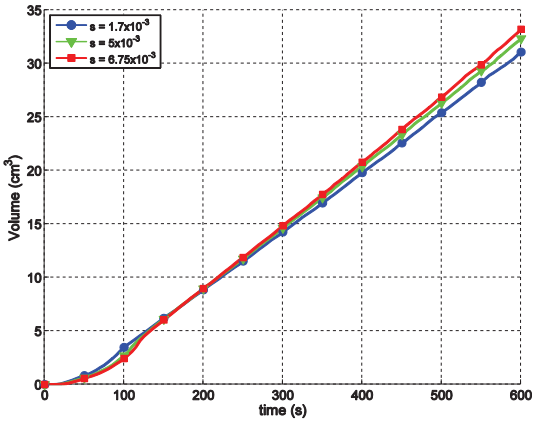

Fig.7. Volumes obtained for $ks = 5$ at 30 V

In Fig.6 and Fig.7, there are shown the values of the volume obtained varying the value of s. As ks and the applied voltage increase, it can be observed that the values of volume obtained for different values of s do not differ significantly. Except for the situation depicted in Fig.6, initially the values obtained with $s = 1.7 \cdot 10^{-3}$ are somewhat larger. As time elapses, the volumes for $s = 6.75 \cdot 10^{-3}$ become bigger, exceeding the values obtained for the other values of s.

Besides the size of the volume of damaged tissue obtained, it is clearly important to understand how the shape of the volume is influenced. It is significant to achieve a regular volume so the tumorous tissue is preferably damaged saving the bile duct from any harm.

Fig.8 presents the volume obtained for voltages from 20 V to 28 V considering $ks = 3$ and $s = 1.7 \cdot 10^{-3}$ after 5 minutes. Same results are depicted in Fig.9, in this case for $s = 6.75 \cdot 10^{-3}$. It can be observed that the ends of the tumour

are at first preferentially heated. Also it can be observed that the volume grows significantly on the opposite side to the blood vessels. Convective heat due to the presence of these major vessels has a significant impact on the shape of the volume obtained. However, the volume is more regular when considering a narrow diffusion of the saline solution in the middle portion of the tumour. This becomes more evident as ks and s increase.

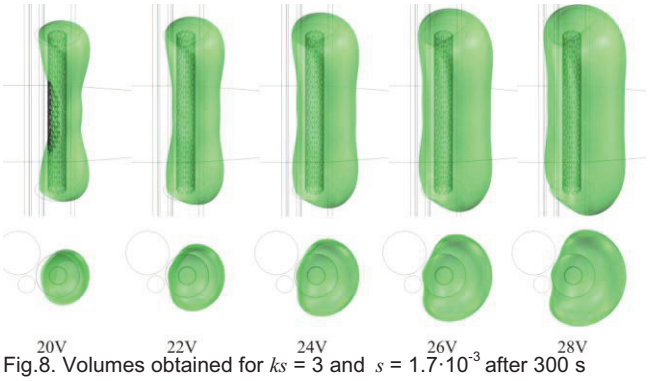

Fig.8. Volumes obtained for ks = 3 and s = $1.7 \cdot 10^{-3}$ after 300 s

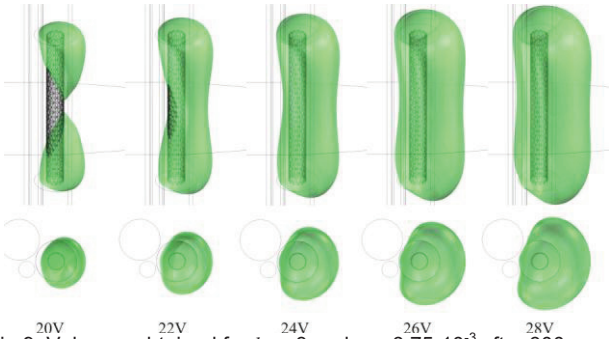

Fig.9. Volumes obtained for ks = 3 and s = $6.75 \cdot 10^{-3}$ after 300 s

Conclusions

As expected, altering the electric conductivity by injecting a saline solution in the middle of the tumour modified the size and the shape of the volume of damaged tissue induced by radio frequency ablation. It was observed that concentration, as well as diffusion of the saline solution along the tumorous tissue, have a significant impact on the shape of the induced lesion. A higher saline solution concentration, ks, associated to a wider diffusion along the tumour, s, lead to a steep heating of the ends of the tumour, thus obtaining an irregular induced lesion. A more regular shape could be achieved considering a relatively low saline solution concentration with a narrow diffusion width, however the blood flow in the porta vein and the hepatic artery still have a significant impact on the final obtained volume.

It should be noticed that, unlike the simplified model considered for the present numerical simulation, the porta hepatis is a more complex structure, with different pulsating blood flows and stroma which was not considered in the present work.

REFERENCES

[1] Gatto M., Bragazzi M.C., Semeraro R., Napoli C., Gentile R., Torrice A., Gaudio E., Alvaro D.: Cholangiocarcinoma: Update and future perspectives, Digestive and Liver Disease, 42(4), pp. 253–260, 2010.

[2] Gatto M., Alvaro D.: New insights on cholangiocarcinoma, World Journal of Gastrointestinal Oncology, 2(3), pp. 136–145, 2010.

[3] Paik W.H., Park Y.S., Hwang J.-H., Lee S.H., Yoon C.J., Kang S.-G., Lee J.K., Ryu J.K., Kim Y.-T., Yoon Y.B.: Palliative treatment with self-expandable metallic stents in patients with advanced type III or IV hilar cholangiocarcinoma: a percutaneous versus endoscopic approach, Gastrointestinal Endoscopy, 69(1), pp. 55–62, 2009.

[4] Antunes C.F.L., Almeida T.R.O., Raposeiro N., Gonçalves B., Almeida P.: Thermal Ablation in Biological Tissue Using Tubular Electrode, 14th Biennial IEEE Conference on Electromagnetic Field Computation, Chicago, USA, 2010.

[5] Antunes C.F.L., Almeida T.R.O., Raposeiro N.: Effects of the Geometry of a Tubular Electrode on the Temperature Distribution in Biological Tissue, 14th Biennial IEEE Conference on Electromagnetic Field Computation, Chicago, USA, 2010.

[6] Antunes C.F.L., Almeida T.R.O., Raposeiro N., Gonçalves B., Almeida P.: Determination of Lesion Volume Induced in Biological Tissue Using a Tubular Electrode for Radiofrequency Ablation – Numerical and Experimental Analysis, EHE2011 - 4th International Conference on Electromagnetic Fields, Health and Environment, Coimbra, Portugal, 2011.

[7] Antunes C.F.L., Almeida T.R.O., Raposeiro N.: Finite Element Modeling of Cholangiocarcinoma Radiofrequency Ablation, 10th International Conference of the European Bioelectromagnetic Association, Rome, Italy, 2011.

[8] Antunes C.F.L., Almeida T.R.O., Raposeiro N.: Inducing Thermal Lesion on a Cholangiocarcinoma Considering a Saline-Enhanced Radiofrequency Ablation, EHE2011 - 4th International Conference on Electromagnetic Fields, Health and Environment, Coimbra, Portugal, 2011.

[9] Plonsey R., Heppner D.: Considerations of quasi-stationarity in electrophysiological systems, Bulletin of Mathematical Biology, 29(4), pp. 657–664.

[10] Pennes H.H: Analysis of Tissue and Arterial Blood Temperatures in the Resting Human Forearm, Journal of Applied Physiololy, 85(1), pp. 5–3, 1998 (reprint).

[11] Arkin H., Xu L.X., Holmes K.R.: Recent developments in modelling heat transfer in blood perfused tissues, IEEE Transactions on Biomedical Engineering, 41(2), pp. 97–107, 1994.

[12] Tziafalia C., Vlychou M., Tepetes K., Kelekis N., V.Fezoulidis I.: Echo-Doppler measurements of portal vein and hepatic artery in asymptomatic patients with hepatitis B virus and healthy adult, Journal of Gastrointestinal and Liver Diseases, 15(4), pp. 343–346, 2006.

[13] Antunes C.F.L., Almeida T.R.O., Raposeiro N., Gonçalves B., Almeida P., Antunes A.: A Tubular Electrode for Radiofrequency Ablation Therapy, World Academy of Science, Engineering and Technology, (70), pp. 517–523, Oct. 2010.

[14] Haemmerich D., Staelin T., Tungjitkusolmun S., Lee F.T., Jr., Mahvi D.M.,Webster J.G.: Hepatic bipolar radio-frequency ablation between separated multiprong electrodes, IEEE T Bio-med Eng, 48(10), pp. 1145–1152, 2001.

[15] Haemmerich D., Staelin S.T., Tsai J.Z., Tungjitkusolmun S., Mahvi D.M., Webster J.G.: In vivo electrical conductivity of hepatic tumours, Physiological Measurement, 24(2), pp. 251–260, 2003.

[16] Haemmerich D., Chachati L., Wright A.S., Mahvi D.M., Lee F.T., Jr.,Webster J.G.: Hepatic radiofrequency ablation with internally cooled probes: effect of coolant temperature on lesion size, IEEE T Bio-med Eng, 50(4), pp. 493–500, 2003.

[17] Goldberg S.N.: Radiofrequency tumor ablation: principles and techniques, European Journal of Ultrasound, 13(2), pp. 129–147, 2001.

***Authors**: Prof. Carlos Lemos Antunes, M.Sc. Nélia Raposeiro, RIANDA Research, Rua Eládio Alle Alvarez, Picoto dos Barbados, 3030-280 Coimbra, Portugal email: lemos.antunes@rianda.pt, M.Sc. Tony Almeida, Departamento de Engenharia Eletrotécnica e de Computadores, Pólo II – Pinhal de Marrocos, 3030–290 Coimbra, Portugal, e-mail: tony@deec.uc.pt*